

Graphene on Ir(111) surface: From van der Waals to strong bonding

R. Brako,¹ D. Šokčević,¹ P. Lazić,² and N. Atodiresei²

¹Rudjer Bošković Institute, 10000 Zagreb, Croatia

²Institut für Festkörperforschung (IFF), Forschungszentrum Jülich, 52425 Jülich, Germany

(Dated: May 28, 2018)

We calculate the properties of a graphene monolayer on the Ir(111) surface, using the model in which the periodicities of the two structures are assumed equal, instead of the observed slight mismatch which leads to a large superperiodic unit cell. We use the Density Functional Theory approach supplemented by the recently developed vdW-DF nonlocal correlation functional. The latter is essential for treating the van der Waals interaction, which is crucial for the adsorption distances and energies of the rather weakly bound graphene. When additional iridium atoms are put on top of graphene, the electronic structure of C atoms acquires the sp^3 character and strong bonds with the iridium atoms are formed. We discuss the validity of the approximations used, and the relevance for other graphene-metal systems.

PACS numbers: 68.43.Bc,

I. INTRODUCTION

Graphene is a one-atom thick two-dimensional structure of carbon atoms arranged in a honeycomb lattice. It is (conceptually at least) at the origin of all other graphitic forms,¹ including the three-dimensional graphite, one-dimensional carbon nanotubes and zero-dimensional fullerenes. The planar geometry and the exceptional strength of graphene² are due to the sp^2 bonds between atoms. Single-layer graphene has been obtained by micromechanical cleavage of graphite and by growth on SiC and metal surfaces. The recent large increase of interest in graphene is due both to the theoretical implications of its unique electronic properties and to its potential applicability, in particular as a novel material for electronics.

As the building block of graphite and as the adsorbate on many surfaces, graphene bonds to its surroundings only weakly, and the character of the bonding is largely van der Waals (vdW). Occasionally, stronger bonding occurs without destroying the geometry of the graphene lattice,³ for example on Ni(111)⁴ and Ru(0001)^{5–7} surfaces. Graphene on Ir(111) is an example where, depending on conditions, both kinds of bonding can occur. Monolayer graphene is vdW physisorbed, and the characteristic graphene lattice can be clearly seen in STM images,⁸ while with additional Ir clusters on top the carbon-metal bonds become stronger.

Large-cell Density Functional Theory (DFT) calculations of graphene on Ir(111) using PBE GGA (Ref. 8) and LDA (Ref. 9) have been performed. However, experiments and calculations reveal a subtle interplay between van der Waals bonding and stronger electronic interaction with the substrate. The vdW interaction is not properly described in the standard local (LDA) and semilocal (GGA) DFT functionals, which provides a serious obstacle to the complete understanding of the nature of the bonding.

In this paper we apply the recently developed extension to the DFT, which replaces the semi-local (i.e. depend-

ing upon the gradient of the electronic density) correlation term with a fully non-local one (depending upon the electronic densities at different points in space), which can describe the van der Waals forces even between two fragments of matter with non-overlapping electronic densities. Due to computational complexity we had to abandon the large supercell which aims to describe more realistically the graphene and Ir(111) surface with their slightly different atomic periodicities, and opt for an approximate description by a smaller commensurate unit cell. While the quantitative accuracy of the results suffers (but we argue that it is a quite limited and controlled problem), the approximation makes the transition from weak to strong bonding easier to analyze and understand.

II. GRAPHENE BINDING IN GRAPHITE

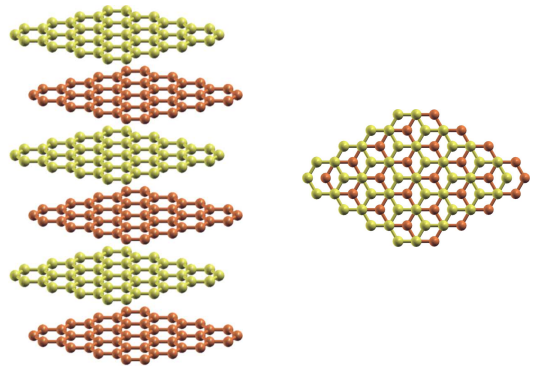


FIG. 1: The structure of graphite, side and top view. The layers are stacked in AB order, so that half of the C atoms lie in chains along the direction perpendicular to the graphene planes, while the other half alternates in the other two high-symmetry positions. The periodicity in the perpendicular direction is c , i.e. the interlayer distance is $c/2$. For clarity, c has been exaggerated by about a factor of 3.

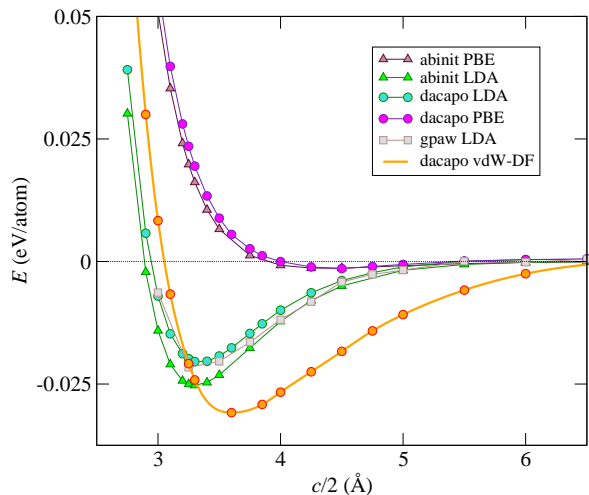


FIG. 2: Binding energies of graphite AB structure as a function of interlayer distance: Comparison of various DFT codes, plane-wave based dacapo¹⁰ and abinit,¹¹ and real-space gpaw.¹² Local LDA and semilocal PBE GGA results are shown. The curve labeled vdW-DF is the energy when the PBE GGA correlation has been replaced by a fully non-local correlation¹³ using the JuNoLo numerical code¹⁴.

We have first applied our methods to graphite, i.e. graphene sheets arranged in the most stable AB stacking, shown in Fig. 1. This is a much studied system with good experimental data and calculated values of structural and energetic parameters. It has the same complexities of having both the weak vdW and strong chemical bonds as our principal subject of interest, graphene on Ir(111). A single sheet of graphene presents no difficulties for the standard DFT GGA approach, giving the C-C distance of 1.42 Å, corresponding to a lattice constant of 2.46 Å, in agreement with the experiment. Next, we performed the Density Functional calculations of stacks of graphene sheets using several flavors of LDA and GGA, implemented in various numerical codes. The calculated cohesive energies are shown in Fig. 2, as a function of the interlayer separation. After that we used the non-local vdW-DF functional for the correlation.^{13,15}

The pure DFT results agree well for all programs used, and are even quite insensitive upon the (lack of) full self-consistency. For example, dacapo calculations use the PW91 GGA functional, but the dacapo LDA curve shown in the figure, obtained evaluating the LDA functional on the electron density calculated with PW91, agrees quite well with the fully selfconsistent abinit LDA results. GGA calculations give little or no bonding, and LDA gives (apparently) reasonable bonding energies and distances, comparable to experimental values. The reason for the failure of GGA is intuitively clear: The semilocal gradient approximation cannot describe well the inherently non-local van der Waals interaction, which exists even between subsystems with completely non-overlapping electronic densities. The apparent success of LDA is somewhat perplexing, since it is even more

local than the more advanced GGA, the latter indeed being more successful when it comes to chemically bound systems. There are strong indications that the agreement of the LDA results is largely fortuitous, as discussed further on.

We have further investigated the problem by applying the vdW-DF theory,¹³ which is at present the most promising approach for treating the non-local correlation. It consists in replacing the semilocal (gradient) part of the GGA correlation functional by a fully non-local term, which still depends only upon the electronic density, in the true spirit of the Density Functional theory. We have applied vdW-DF as implemented in the JuNoLo code¹⁴ in a post-processing approach, i.e. we used the electron densities obtained in the standard GGA calculation to evaluate the non-local vdW-DF correlation, and inserted it into the total energy instead of the semilocal correlation. This approach is, of course, not fully selfconsistent, since the DFT potential and the Kohn-Sham wavefunctions, and hence the electron density can depend upon the details of the correlation functional used. However, a recent selfconsistent implementation of the vdW-DF correlation functional shows that the differences are negligible.¹⁶ We have therefore relied on the post-processing approach which is less time consuming and avoids any intervention in the code of the DFT programs. Changing the correlation contribution changes the total energy, and therefore the forces acting on the atoms as well. However, all atomic configurations which we consider here have high symmetry, where we can sweep the interesting range of interlayer separation “by hand” in order to find the optimum configuration. The lack of fully selfconsistent atomic relaxations inherent to such an approach is not a major problem, as discussed later on. We furthermore note that we have not followed the suggestion put forward by the authors of the vdW-DF theory to use the revPBE exchange functional,¹³ and have instead continued using the PBE exchange. Although revPBE exchange seems to compensate for too large binding energies for several van der Waals bound systems, it gives worse equilibrium distances, and the same improvement does not seem to occur in cases of strong bonding.

The vdW-DF results shown by a thick line in Fig. 2 are qualitatively similar to the LDA results, but with some important differences. The equilibrium distance at around 3.6 Å is larger than the LDA result, as is the binding energy of 30.8 meV per carbon atom. The vdW-DF attractive potential has clearly a longer range than LDA, which reflects the long-range nature of the van der Waals attraction and reveals the fortuitous character of the agreement with LDA around the minimum. The vdW-DF values for the interlayer separation and interaction energy agree well with recent experimental results and theoretical calculations (See Ref. 17 and references therein). Recently, it has been found that the behavior of the nonretarded van der Waals interaction between nonoverlapping anisotropic nanostructures that have a zero electronic energy gap should be different than pre-

dicted from the the usual sum of R^{-6} contributions,¹⁸ but this is probably relevant only in the extreme asymptotic regime.

We conclude that the inclusion of the van der Waals interaction is essential to reproduce physical properties of graphite, and that the vdW-DF approach successfully treats all aspects of the graphene binding in graphite.

III. STRUCTURE OF GRAPHENE ON Ir(111) SURFACE

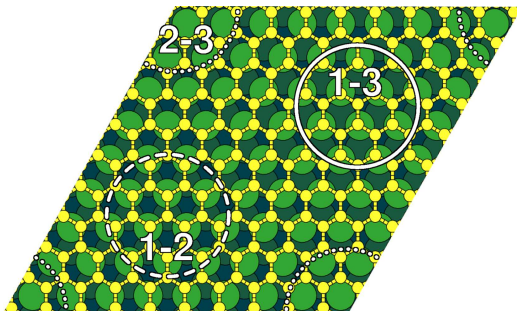


FIG. 3: Moiré superstructure of 10×10 graphene on 9×9 Ir(111) unit cell. The C atoms are (approximately) above the first and third layer Ir atoms within the circle labeled 1-3, above the first and second layer in 1-2, and above the second and third layer in 2-3.¹⁹

Graphene monolayers of high structural quality, extending over tens of nanometers and even up to micrometer size, orientationally well aligned with the substrate, have recently been obtained by hydrocarbon decomposition on Ir(111).⁸ The lattice constants of graphene and the Ir(111) surface differ at room temperature by around 10%, and the STM micrographs clearly show the moiré pattern due to the lattice mismatch. In Fig. 3 the supercell with a 10×10 graphene lattice on top of 9×9 structure of iridium atoms is shown. A further intriguing feature is observed when additional iridium atoms are adsorbed on top of the graphene. STM images show that the adatoms form regular arrays on clusters, selectively bound to certain regions of the moiré pattern.^{8,9}

Density functional calculations employing the PBE GGA functional⁸ and LDA functional⁹ on a supercell similar to the one in Fig. 3 have been performed. It has been found that the PBE GGA functional gives almost no bonding of graphene monolayer on Ir(111) (Refs. 8 Erratum, 20), while the LDA functional gives reasonable results for bonding energies and interatomic distances, both without and with additional clusters on top.⁹ These results are qualitatively reminiscent of our results for graphite, i.e. we again see an apparent success of the quite basic LDA, which signals that a more detailed investigation is necessary.

Our strategy is similar to the approach used for graphite in Section II. We start with the standard DFT

and later investigate the effects of the non-local correlation. We do not use the realistic large unit cell shown in Fig. 3, but instead we compress the Ir(111) substrate in the surface plane (coordinates x, y) so that it matches the lattice constant of graphene. By changing the phase of the carbon atoms with respect to the underlying lattice of Ir atoms, we are able to simulate (approximately) any point in the supercell in Fig. 3. We have done most calculations for the region labeled 1-3, which both experiment and calculations show to be the most strongly bonding, with only a few checks of the other regions.

Calculations of commensurate graphene-metal surface systems has been done for several metal surfaces, either by adjusting the substrate lattice constant²¹ or the graphene lattice constant²². We shall discuss these calculations into more detail later on.

The mismatch of the lattice constant of graphene (2.46 Å) and that of the Ir(111) surface (2.73 Å, corresponding to the conventional fcc lattice constant $a_0 = 3.86$ Å) is around 10%, clearly larger than those in Ref. 21, which are in the range of 0.8-3.8%. In order to minimize possible artefacts due to the squeezing of the iridium substrate to fit the graphene lattice we optimized the lattice constant of the iridium substrate in the z direction. To that end, we performed calculations of iridium bulk with compressed (111) planes and allowed it to relax in the perpendicular direction. The lattice constant in the z direction increased by about 10% to 4.24 Å, and we used this lower-symmetry iridium lattice, compressed in $x - y$ directions and expanded in z , as the substrate in our calculations. From the point of view of quantitative accuracy, a calculation using a large supercell and “natural” iridium substrate would be preferred, but our approach enables a clear insight into the bonding properties, which would be at risk to remain buried and hard to see in a more realistic large calculation.

Another important aspect of graphene interaction with the Ir(111) surface can be inferred from the band structure of Ir(111) along high-symmetry directions of the surface Brillouin zone. Our calculations based on the DFT Kohn-Sham eigenstates²³ as well as ARPES experiments^{23,24} show that there is an energy gap around the K point of the surface Brillouin zone, extending from just below the Fermi level down to almost 1.5 eV binding energy. The vertex of the “Dirac cone” of the π bands of graphene adsorbed on Ir(111) lies entirely within this gap.²⁴ The weak interaction of graphene with the iridium substrate can be attributed to this mismatch of the electronic states, since the unsaturated π bands of the Dirac cones don’t have any substrate states with the same momentum k and energy E to hybridize with. We have also checked the band structure of our compressed iridium surface and found that the band gap around the K point is still present and has a similar shape, which implies that the weak character of the graphene interaction with Ir(111) will not be much affected by the use of the compressed substrate.

In our DFT calculations we use a three-layer Ir(111)

slab with the adjusted lattice constants in the $x - y$ and the z directions as explained above. It would have been easy to use a thicker substrate, but this would add no further quantitative accuracy, considering other simplifications and approximations used.

IV. DFT CALCULATIONS OF GRAPHENE ON Ir(111) AND Ir-GRAPHENE-Ir SANDWICHES

For our calculations we have chosen four characteristic structures of graphene on iridium, shown in Fig. 4. The structures are periodic in the $x - y$ plane and extend to infinity, but for clarity we show only a small symmetric cluster of atoms for each one. There are two atoms in the unit cell of graphene, which in the following we denote by C_A and C_B , as illustrated in Fig. 4 (d). We denote the iridium atoms in the first substrate layer by Ir_S , and the atoms in the first overlayer as Ir_O .²⁵

The structures were chosen so that they illustrate Ir-C bonds of various character, with overall bonding strength increasing from structure (a) to structure (d). The iridium substrate is modeled by three atomic layers in all cases. The structures are: (a) Monolayer graphene on Ir(111) with C_A above Ir_S and C_B above third layer Ir, which illustrates the most stable regions of the moiré pattern of a monolayer graphene on Ir(111); (b) Graphene monolayer as in (a), but with a single overlayer of iridium atoms, with Ir_O located above the centers of the hexagonal rings of the graphene; (c) Three additional layers of iridium, with Ir_O above C_B ; (d) A single Ir overlayer, with atoms in the same positions as in the first layer in (c). In (c) and (d) there is one iridium atom below C_A and another one above C_B , which models the geometries of the stable iridium clusters on top of graphene observed in the experiment.

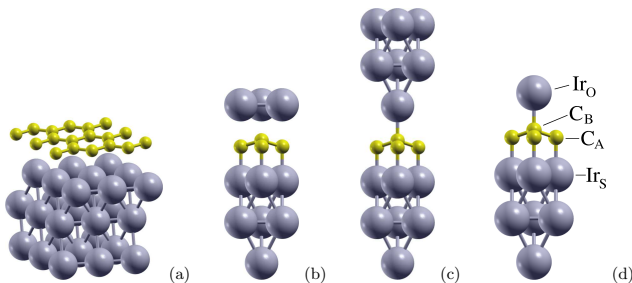


FIG. 4: The four structures considered in the paper. For clarity, only a few atoms from each atomic layer are shown in structures (b)-(d).

A. Standard DFT only

We first calculated the dependence of the interaction energy upon Ir-graphene separation for structures (a)-(d), using the standard LDA and GGA PBE functionals.

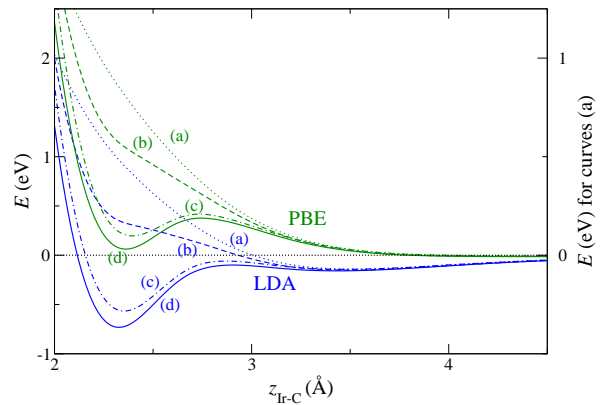


FIG. 5: DFT (LDA and PBE GGA) energies for graphene on Ir, structure (a) in Fig. 4, and Ir-graphene-Ir sandwiches, structures (b)-(d) in Fig. 4. In this and the following graphs the energies are given per unit cell, i.e. two C atoms and one Ir atom in each iridium layer.

The results are shown in Fig. 5. Two comments are in order. For structure (a), the energy scale in Fig. 5 is smaller by a factor of two, since the graphene has iridium atoms only on one side, and the interaction (in particularly the repulsion at small distances) is expected to scale with the number of neighboring atomic planes. Secondly, for the sandwich structures (b)-(d) the graphene layer was at the beginning of the calculations placed symmetrically between the nearest Ir layers, each of them at a distance of z_{Ir-g} , but was allowed to relax in the course of the calculation. At small separations z_{Ir-g} the graphene buckles, with C_A atom moving towards Ir_S and C_B towards the overlayer. This is not a major problem, since the two atoms move by almost the same amount in opposite direction, even in the case of the less symmetrical structure (b), so that z_{Ir-g} still measures the z -averaged position of the graphene plane. There is no buckling at z_{Ir-g} separations larger than say 3 Å. Since the relaxation was done according to the forces calculated in GGA functional, which does not develop any appreciable attractive potential well at these distances, there was no danger that the graphene layer would be attracted to the iridium atoms on one side. Iridium atoms were not relaxed.

The results for all structures almost coincide for z_{Ir-g} larger than around 3.3 Å, for both GGA and LDA, i.e. the interaction at physisorption distances does not show a large corrugation along the $x - y$ coordinates. The sandwich structures (b)-(d) show the tendency to form a strong bond at small graphene-Ir distances. The minimum is around 2.3 Å, and is quite sensitive on the relative position of the atoms in the $x - y$ plane. Thus in the unfavorable structure (b), where the Ir atoms in the additional layer do not lie directly above the C atoms, there is only a kink in the interaction energy at about 2.3 Å, hinting that there is a tendency towards strong chemical bonding. The structures (c) and (d) develop a

distinct potential well around that distance, which is not deep enough in the PBE GGA functional calculation, but with the LDA functional it becomes the stable configuration with more than 0.5 eV binding energy. Note that the quantity $z_{\text{Ir-g}}$ measures the distance to the average z coordinate of the graphene layer, and since there is a buckling of about 0.2 Å of C atoms towards the nearest Ir atom, the Ir-C distance is actually around 2.1 Å, as discussed more into details later on.

These results prompt us to reevaluate even the standard DFT calculations in the region of strong bonding at small Ir-C distances, where the graphene layer significantly changes its electronic character. Up to now we have consistently used the lattice constant of free graphene, assuming that it is optimal for the bound system too (and we went to the trouble of compressing the Ir layers accordingly). This may not be true in the region of strong bonding, and we first check this.

To that end, we performed standard DFT calculations of structures (c) and (d) with the lattice constant in the $x-y$ plane slightly expanded from the value of free graphene (3.478 Å, C-C distance 1.42 Å) and accordingly reduced in the z direction, and checked whether there was any improvement of the total energy. In order to evaluate the bonding energy we also had to calculate the energy of separated Ir and graphene slabs (corresponding to $z_{\text{Ir-g}} \rightarrow \infty$) for each value of the expanded lattice constant, and subtract it from the energy of the interacting system. In Fig. 7 we show the results for structures (c) and (d). The unconnected circles are the non-optimized results for the two structures taken from Fig. 5, while the connected circles are the best results obtained by expanding the lattice. We see that the energy improves significantly in the region of strong bonding, where the optimum lattice constant at the position of the minimum, $z_{\text{Ir-g}} \sim 2.3$ Å, increases from the free graphene value of 3.478 Å to 3.65 Å for structure (c) and to 3.72 Å for structure (d). The fact that in the region of weak binding, for $z_{\text{Ir-g}} > 3$ Å, there is no improvement of energy and the optimal lattice constant remains at the value of free graphene (i.e. the large graphene stiffness dominates the energy balance) indicates that the procedure of optimizing the lattice constant is consistent with other approximations used in the calculations.

B. DFT with vdW-DF

In order to account for the van der Waals interaction and the effects of the long-range correlation in general, we applied the vdW-DF approach in a post-GGA procedure to DFT results for the structures (a), (c) and (d). Here the full power of the vdW-DF correlation approach becomes obvious, because due to its “seamless” character we can apply it at all graphene-Ir distances, i.e. at all coupling strengths, without worrying that it may spoil the GGA results which are good for strong bonding.²⁶

The results for structure (a) are shown by squares in

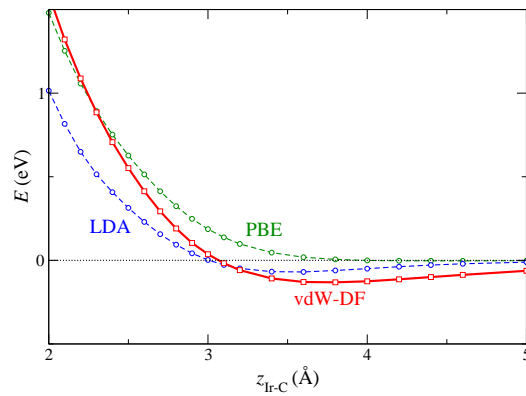


FIG. 6: Standard DFT (LDA and PBE GGA) and vdW-DF energies for graphene monolayer on Ir(111), structure (a) in Fig. 4.

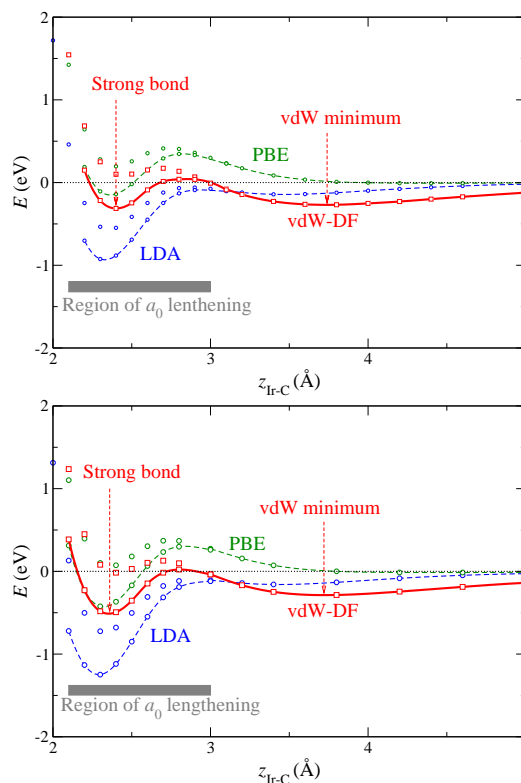


FIG. 7: Standard DFT (LDA and PBE GGA) and vdW-DF energies for Ir-graphene-Ir sandwiches, structures (c) and (d) in Fig. 4. The lines connect points for which the energy has minimum when allowing the structures to slightly expand laterally, as explained in the text.

Fig. 6, where the PBE and the LDA results are the same as in Fig. 5, and the energy calculated using vdW-DF is shown by a thick line and squares. A clear van der Waals attractive well develops, deeper than the shallow well in the LDA calculation, and with the minimum at a larger graphene-substrate distance, around 3.7 Å. Fig. 7 shows similar results for structures (c) and (d). The unconnected points are for the lattice constant of free

graphene, as in Fig. 5, and the points connected by lines for the optimized expanded lattice constant. The van der Waals potential well is similar to Fig. 6 but approximately two times deeper (note the different scale on the energy axis), since the graphene interacts both with the iridium substrate and overlayer. The depth and shape of the chemisorption minimum at around 2.3 Å is less affected, but the barrier between the two minima is much decreased compared with the DFT results.

C. Discussion of the results

Detailed information about the nature of C–C and C–Ir bonds can be inferred by examining the geometry of the graphene lattice around the minima of the interaction energy in Fig. 7. At the physisorption minimum, $z_{\text{Ir-g}} \sim 3.7$ Å, the graphene lattice is perfectly planar, and the graphene stays at midpoint between two neighboring iridium layers. The same is true for all structures in Fig. 4, and in fact for other geometries such as monolayer graphene over the 1-2 and 2-3 regions in Fig. 3. Due to the smoothness of the potential with respect to the translation of graphene along the surface, graphene flakes physisorbed on Ir(111) are quite mobile, both translationally and rotationally, which is an important mechanism in aggregation and growth of large graphene islands.²⁷

| Structure | a_0 | $z_{\text{S-A}}$ | z_{buck} | $z_{\text{B-O}}$ | $d_{\text{A-B}}$ | α |
|-----------|-------|------------------|-------------------|------------------|------------------|----------|
| (c) | 3.65 | 2.17 | 0.40 | 2.17 | 1.54 | 105° |
| (d) | 3.72 | 2.22 | 0.41 | 2.17 | 1.57 | 105.3° |

TABLE I: Bond length and angles at the strong bonding energy minima of structures (c) and (d). All lengths are in Å. Here a_0 is the optimal lattice constant of the structure in the $x-y$ plane, slightly larger than the free graphene value of 3.478 Å, $z_{\text{S-A}}$ is the distance between the substrate atom Ir_S and C_A, z_{buck} is the buckling of graphene, i.e. the difference of z coordinates of atoms C_A and C_B, $z_{\text{B-O}}$ the distance between C_B and the overlayer atom Ir_O, $d_{\text{A-B}}$ the distance between two neighboring C atoms, and α the angle defined by the lines Ir_S–C_A and C_A–C_B.

The situation is rather different when strong bonding between iridium and graphene in Ir-graphene-Ir structures occurs, at $z_{\text{Ir-g}}$ around 2.3 Å in Fig. 7. First, we notice that the total energy depends strongly on the position of the C atoms of graphene with respect to the Ir atoms below and above. Thus the two similar structures, (b) and (d) in Fig. 4, differ only in the position of the iridium atoms in the monoatomic overlayer, but the total energies in Fig. 5 differ by more than 1 eV! The absence of a stable strong bond in structure (b) shows that strong bonding can occur only when both C atoms are saturated by Ir atoms, one directly below and one above it. This immediately implies that the onset of strong bonding effectively anchors the iridium cluster and the underlying

graphene to the particular spot of the moiré pattern of the graphene-substrate supercell.

The formation of the strong “organometallic” bond is accompanied by buckling of graphene and C–C bond lengthening. Table I shows the values of bond lengths and angles corresponding to the strong bonding energy minima in the two panels of Fig. 7. These values are close to the ones of the tetrahedrally bonded C atoms in diamond, and indicate that the rehybridization from sp^2 to sp^3 bonding has occurred, as noted by Feibelman.⁹

V. DISCUSSION

These results show that the onset of the strong C–Ir binding in Ir-graphene-Ir sandwiches is accompanied by the disappearance of the aromatic character of the carbon rings. The carbon atoms rehybridize to sp^3 configuration, and the two C atoms in the graphene unit cell move out of the plane in opposite directions. On the other hand, in one-sided binding on Ir(111) (i.e. a clean graphene overlayer) the C–Ir bond is always weak, dominated by van der Waals interaction.

In order to get more insight into the character of the bonding of aromatic rings on Ir(111), we have made DFT calculations of benzene molecules C₆H₆ lying flat on the iridium surface. We found large differences of binding energies and distances for different positions of the benzene molecules with respect to the substrate atoms. The most stable configuration is when the center of the ring is above a hollow site, and the six C atoms are above three Ir atoms, two C on each Ir. (This configuration cannot be directly compared to any part of the moiré pattern of graphene on Ir(111), Fig. 3, since it corresponds to a different orientation of the aromatic rings, i.e. rotated by 30°.) The C–Ir bond is around 2.4 Å. The GGA adsorption energy is somewhat less than 1 eV, and does not change substantially when the vdW-DF nonlocal correlation is used. The C atoms remain planar due to symmetry, but the C–C bonds become longer, 1.43 Å and 1.48 Å, and the H atoms are slightly above the plane of the C atoms. This indicates a change of the nature of the bonding of the carbon ring and a departure from the pure sp^2 hybridization. The configurations where the center of the benzene ring is above an Ir atom, and H atoms point either towards the neighboring Ir atoms or towards bridge sites, are more weakly bound. The C–Ir bond length is around 3.4 Å. In this case the nonlocal correlation is essential for the bonding. With pure GGA functional there is virtually no bonding of the benzene molecule, while with the vdW-DF the bonding energy is around 0.6 eV. The C–C bonds keep the value of 1.41 Å as in the benzene molecule, and the whole benzene structure is planar. These values are also very similar to those of graphene on Ir(111) obtained earlier. All these results indicate a weak, van der Waals-dominated bonding. Thus the bonding of benzene on Ir(111) shows even more variation of bonding parameters than various re-

gions of the moiré of graphene, indicating the richness of possible bonding of aromatic structures (molecules and graphene) on metal surfaces.

Graphene strongly binds on some other surfaces, as mentioned in the Introduction, apparently without strong rehybridization to sp^3 . In a recent combined experimental and theoretical study of graphene bonding on Ru(0001) surface,⁷ it was found that graphene is strongly corrugated with a minimum C-Ru distance of 2.1 Å and a corrugation of 1.53 Å in the regions of strong coupling. The DFT calculations were performed using the standard PBE functional, which is expected to work well in the regions of strong coupling, and the lack of the van der Waals interaction which should be dominant in the weakly coupled ‘blisters’ is not crucial. The authors find that the height difference between neighboring C atoms in the graphene layer is below 0.03 Å in the strong coupling region in DFT, and conclude that the adsorbed graphene layer remains sp^2 hybridized.

Returning to the calculations of graphene on Ir(111), we note that the use of the large supercell in Ref. 9 has the advantage that the lattice constants of both the iridium substrate and the graphene overlayer can be kept close to their natural values. Thus the problems which we encounter with our compressed Ir surface (expanded in the z direction) are avoided. In particular, it seems that we get somewhat too large Ir-graphene distances compared to other calculations and the preliminary experimental estimates. Furthermore, when iridium clusters are added on top of graphene, in the large supercell approach the carbon atoms are free to relax both vertically and laterally, which is essential for a good description of graphene buckling and the formation of the strong C–Ir bond. In subsection IV B we had to use a calculational tour de force to detect the preference of carbon atoms to lengthen somewhat the C–C bonds and thus approach more closely the diamond structure. Furthermore, in the supercell approach the substrate iridium atoms may also relax laterally, optimizing the saturation of the bonds to carbon atoms.

These advantages come with the downside that in Ref. 9 the LDA functional was used. This was a necessary choice since GGA in the usual formulation, i.e. without the van der Waals interaction being somehow accounted for, gives little or no binding of graphene (see Ref. 8, in particular the Erratum). However, LDA usually gives a too small equilibrium distance, and overbinds in cases of strong chemical bonding. Thus in our calculations of graphite in section II, Fig. 2, LDA gave a too small interlayer distance. The LDA binding energy of graphite was also too small since graphite is a system with very little chemical component of the bond and the LDA overbinding could not compensate fully the absence of the vdW component.

The compressed Ir(111) surface in our approach and the use of LDA in Ref. 9 preclude a detailed quantitative comparison between the results of the two calculations, and of each of them with experiment. However, the semi-

quantitative agreement is good. Both approaches predict a rather weak bonding of a graphene monolayer with the Ir(111) substrate, and the formation of a much stronger organometallic bond when iridium clusters are added on top, accompanied with the buckling of the graphene structure and shortening of Ir–C distances. For clean graphene, the Ir–C separation at the 1-3 regions of the moiré pattern is around 3.48 Å in Ref. 9 and around 3.7 Å in our work, while the experimental value has been estimated to around 3.38 Å. When the clusters trigger strong bonding and graphene buckling the Ir–C distance decreases to around 2.1 Å in Ref. 9 and to around 2.2 Å in our work, while the Ir–C–C angles are around 105°.

The bonding of graphene on some other (111) surfaces of fcc metals assuming commensurate configurations has also been investigated. In the papers by Giovannetti et al.²¹ and Khomyakov et al.,²⁸ the LDA functional was used. The unit cells were either 2 graphene C atoms and one metal atom in each layer (e.g. Ni, Co, Cu), as in our calculation, or 8 C atoms and 3 metal atoms with the graphene unit cell rotated by 30° when the difference of the lattice constants was larger (e.g. Pd, Au, Pt). It was found that graphene interacts strongly with Ni, Co, and Pd, with the equilibrium metal-graphene distance between 2.05 and 2.30 Å, and weakly with Cu, Au and Pt, with equilibrium distance between 3.26 and 3.31 Å. These findings are in agreement with experiment, where available. The mismatch of the lattice constant of graphene is 4% for Cu, 1.2% for Ni and 2% for Co (metal unit cell being larger in all three cases). This is clearly smaller than in our calculation, where the difference of Ir(111) and graphene lattice constants is around 10%.

Vanin et al.²² consider the same surfaces, but in a quite different approach. They use the vdW-DF correlation functional¹³ evaluated using the method proposed in Ref. 29 and self-consistently implemented into the real-space projector augmented wave gpaw code.¹² They do not adjust the metal substrate to match the lattice constant of graphene, but instead keep it at their experimental lattice parameters and adjust the graphene sheet. They claim that the vdW-DF results do not change significantly if they fix the graphene lattice parameter to its optimized value and adjust the metals correspondingly. Surprisingly, they obtain weak binding for all metals considered, with metal-graphene distances in the range 3.40–3.72 Å. This is in clear disagreement for Co and Ni, where strong binding has been experimentally confirmed.

In contrast to this, our calculations of Ir(111)-graphene structures give an overall agreement with other calculations and with experiment. The weak vdW minimum around 3.7 Å which exist both for clean graphene overlayer (Fig. 6) and for graphene with iridium adclusters (Fig. 7) is obtained correctly only with vdW-DF. The overall shape of the potential minimum of the strong bond around 2.3 Å for iridium adclusters is roughly similar for calculations using LDA and PBE with vdW-DF, although LDA clearly overbinds. Even plain PBE calculations show a comparable local minimum, just weaker.

The disagreement found in Ref. 22 is therefore even more surprising. We have not tried our method on metals other than iridium, where the strong chemisorption minimum exists only if adclusters are present. There is a possibility that vdW-DF does not work so well for other metals. However, in our opinion the source of disagreement may also be the other approximations used in Ref. 22.

The graphene is particularly stable due to the aromatic character of the carbon rings. Perturbing the structure (for example by forcibly changing the natural bond length) may significantly change the reactivity. Thus simply adapting the graphene lattice constant to the substrate may have unwanted consequences, weakening the stability of the aromatic bonds, as well as changing the doping of the graphene layer in contact with the metal surface. The opposite procedure, which we used in this paper, i.e. adapting the substrate lattice constant, seems preferable to us but may also have some weaknesses. First, the change of the electronic structure of the substrate may be large enough to alter the reactivity compared to the natural metal. Also, the lattice constant of the free graphene may not be optimal for rehybridized graphene forming strong sp^3 bonds. We had to expand the graphene lattice slightly in order to obtain a sufficiently stable strong bonding. In the process we had to carefully account for the change in energy of the iridium substrate, which was, of course, also expanded (i.e. less compressed compared to the natural structure). All this indicates that the graphene lattice constant should be left at its natural value in the weak bonding cases, but should be allowed to relax and lengthen when the strong bonding regime accompanied with graphene buckling and rehybridization to diamondlike bond occurs. This cannot be achieved in the simplified commensurable geometries, and a full large supercell calculation with state-of-the-art

nonlocal correlation functional seems to be the only approach which can give the answer about the structure of graphene adsorbed on various metals in the general case.

VI. CONCLUSIONS

We find that a graphene monolayer on Ir(111) is weakly bound, and keeps the aromatic character of the carbon rings. In Ir-graphene-Ir structures C atoms show a tendency towards rehybridization and formation of sp^3 bonds, which in favorable cases (an Ir atom directly below or above each C atom) are more stable than the physisorbed structure. In all cases, the use of the vdW-DF which includes a full description of the nonlocal correlation is essential. However, our approach in which the substrate lattice constant is adjusted to match graphene does not give full quantitative accuracy. In order to obtain that kind of agreement, large calculations on realistic supercells using DFT functionals with nonlocal correlation are necessary. This conclusion is also true for other graphene-on metal systems, in which the nature of the graphene-metal bond may be quite different than on Ir(111).

Acknowledgments

This work was supported by the Ministry of Science, Education and Sports of the Republic of Croatia, under Contract No. 098-0352828-2863. P. Lazić acknowledges the financial support from Alexander von Humboldt foundation.

-
- ¹ A. K. Geim and K. S. Novoselov, *Nature Mater.* **6**, 183 (2007).
- ² C. Lee, X. Wei, J. W. Kysar, and J. Hone, *Science* **321**, 385 (2008).
- ³ J. Wintterlin and M.-L. Bocquet, *Surface Sci.* **603**, 1841 (2009).
- ⁴ G. Bertoni, L. Calmels, A. Altibelli, and V. Serin, *Phys. Rev. B* **71**, 075402 (2004); M. Fuentes-Cabrera, M. I. Baskes, A. V. Melechko, and M. L. Simpson, *Phys. Rev. B* **77**, 035405 (2008).
- ⁵ S. Marchini, S. Günther, and J. Wintterlin, *Phys. Rev. B* **76**, 075429 (2007);
- ⁶ D. Martoccia, P. R. Willmott, T. Brugger, M. Björck, S. Günther, C. M. Schlepütz, A. Cervellino, S. A. Pauli, B. D. Patterson, S. Marchini, J. Wintterlin, W. Moritz, and T. Greber, *Phys. Rev. Lett.* **101**, 126102 (2008);
- ⁷ W. Moritz, B. Wang, M.-L. Bocquet, T. Brugger, T. Greber, J. Wintterlin, and S. Günther, *Phys. Rev. Lett.* **104**, 136102 (2010).
- ⁸ A. T. N'Diaye, S. Bleikamp, P. J. Feibelman, T. Michely, *Phys. Rev. Lett.* **97**, 215501 (2006); **101**, 219904(E) (2008).
- ⁹ P. J. Feibelman, *Phys. Rev. B*, *Phys. Rev. B* **77**, 165419 (2008).
- ¹⁰ <https://wiki.fysik.dtu.dk/dacapo/>
- ¹¹ X. Gonze, J.-M. Beuken, R. Caracas, F. Detraux, M. Fuchs, G.-M. Rignanese, L. Sindic, M. Verstraete, G. Zerah, F. Jollet, M. Torrent, A. Roy, M. Mikami, Ph. Ghosez, J.-Y. Raty, and D. C. Allan, *Comput. Mater. Sci.* **25**, 478 (2002); The ABINIT code is a collaborative project of the Université Catholique de Louvain, Corning, Inc., and other collaborators; <http://www.abinit.org/>
- ¹² J. J. Mortensen, L. B. Hansen, and K. W. Jacobsen, *Phys. Rev. B* **71**, 035109 (2005); <https://wiki.fysik.dtu.dk/gpaw/>
- ¹³ M. Dion, H. Rydberg, E. Schröder, D. C. Langreth, and B. I. Lundqvist, *Phys. Rev. Lett.* **92**, 246401 (2004); **95**, 109902(E) (2005).
- ¹⁴ P. Lazić, N. Atodiresei, M. Alaei, V. Caciuc, S. Blügel, and R. Brako, *Comput. Phys. Commun.* **181**, 371 (2010); <http://www.fz-juelich.de/iff/src/th1/JuNoLo/>
- ¹⁵ For a review of the work of the authors of vdW-DF see:

- D. C. Langreth, B. I. Lundqvist, S. D. Chakarova-Käck, V. R. Cooper, M. Dion, P. Hyldgaard, A. Kelkkanen, J. Kleis, Lingzhu Kong, Shen Li, P. G. Moses, E. Murray, A. Puzder, H. Rydberg, E. Schröder, and T. Thonhauser, J. Phys.: Condens. Matter **21**, 084203 (2009).
- ¹⁶ T. Thonhauser, V. R. Cooper, S. Li, A. Puzder, P. Hyldgaard, and D. C. Langreth, Phys. Rev. B **76**, 125112 (2007).
- ¹⁷ L. Spanu, S. Sorella, and G. Galli, Phys. Rev. Lett. **103**, 196401 (2009).
- ¹⁸ J. F. Dobson, A. White, and A. Rubio, Phys. Rev. Lett. **96**, 073201 (2006).
- ¹⁹ The regions which we denote by 1-3, 1-2, and 2-3, are called ‘hcp’, ‘fcc’, and ‘atop’ regions in Refs. 8 and 9, according to the Ir(111) high-symmetry site which is surrounded by C-atom rings, i.e. which is *not* covered by a graphene atom.
- ²⁰ P. Lacovig, M. Pozzo, D. Alfè, P. Vilmercati, A. Baraldi, and S. Lizzit, Phys. Rev. Lett. **103**, 166101 (2009).
- ²¹ G. Giovannetti, P. A. Khomyakov, G. Brocks, V. M. Karpan, J. van den Brink, and P. J. Kelly, Phys. Rev. Lett. **101**, 026803 (2008).
- ²² M. Vanin, J. J. Mortensen, A. K. Kelkkanen, J. M. Garcia-Lastra, K. S. Thygesen, and K. W. Jacobsen, Phys. Rev. B **81**, 081408(R) (2010).
- ²³ I. Pletikosić, M. Kralj, D. Šokčević, R. Brako, P. Lazić, and P. Pervan, J. Phys.: Condens. Matter **22**, 135006 (2010).
- ²⁴ I. Pletikosić, M. Kralj, P. Pervan, R. Brako, J. Coraux, A. T. N’Diaye, C. Busse, and T. Michely, Phys. Rev. Lett. **102**, 056808 (2009).
- ²⁵ The labels A and B for the two inequivalent sublattices of graphene is not to be confused with the same letters used to denote the graphene stacking in Section II. Both notations are widely used.
- ²⁶ In fact, in some cases the non-local correlation makes crucial improvements to the description of strongly bound systems, as has been recently shown for the known ‘puzzle’ of CO chemisorbed on transition metal surfaces, P. Lazić, M. Alaei, N. Atodiresei, V. Caciuc, R. Brako, and S. Blügel, Phys. Rev. B **81**, 045401 (2010).
- ²⁷ J. Coraux, A. T. NDiaye, M. Engler, C. Busse, D. Wall, N. Buckanie, F.-J. Meyer zu Heringdorf, R. van Gastel, B. Poelsema, and T. Michely, New Journal of Physics **11**, 023006 (2009).
- ²⁸ P. A. Khomyakov, G. Giovannetti, P. C. Rusu, G. Brocks, J. van den Brink, and P. J. Kelly, Phys. Rev. B **79**, 195425 (2009).
- ²⁹ G. Román-Pérez and J. M. Soler, Phys. Rev. Lett. **103**, 096102 (2009).